The gravitomagnetic vector potential and the gravitomagnetic field of a rotating sphere

Jacob Biemond*

Vrije Universiteit, Amsterdam, Section: Nuclear magnetic resonance, 1971-1975
**Postal address: Sansovinostraat 28, 5624 JX Eindhoven, The Netherlands*
Website: http://www.gravito.nl/ Email: j.biemond@gravito.nl

ABSTRACT

The gravitomagnetic vector potential and corresponding gravitomagnetic field generated by a rotating sphere with a homogeneous mass density are investigated. Outside the sphere both vector potential and field may coincide with the results from the ideal dipole model. For the axial gravitomagnetic field inside the sphere a new exact expression is derived.

More general expressions for both vector potential and field inside the sphere are proposed and checked. Their validity is compared with series expansions for the equatorial gravitomagnetic vector potential and gravitomagnetic field. Application of Stokes' theorem to the basic gravitomagnetic equation is compatible with the ideal dipole result for the gravitomagnetic field at the surface of the sphere. Starting from the basic gravitomagnetic equations, the validity of the general internal gravitomagnetic field is confirmed. Observations of two LAGEOS satellites, Gravity Probe B mission and planned ring-laser experiment are shortly discussed.

Starting from the Maxwell equations, the present treatment can also be applied to the electromagnetic case. Analogous results are found for the electromagnetic vector potential and the electromagnetic field.

1. INTRODUCTION

The analogy between the magnetic field generated by moving charge and a so-called "magnetic-type" gravitational field generated by moving mass has been noticed by many authors. For this reason, e.g., Heaviside [1], Singh [2], and Cattani [3] already proposed Maxwell-type gravitational equations. Several deductions of the gravito-magnetic equations, analogous to the Maxwell equations, has been introduced later on in the development of the theory of general relativity. Starting from the Einstein equations in the slow motion and weak field approximation, Peng [4], Biemond [5, 6, 7], Ruggiero and Tartaglia [8] and many others deduced a set of four differential equations.

In the stationary case the gravitomagnetic field **B** can be obtained from the following gravitomagnetic equations [5, 6, 7]

$$\nabla\times\mathbf{B} = -4\pi\beta c^{-1}G^{1/2}\rho\,\mathbf{v} \quad \text{and} \quad \nabla\cdot\mathbf{B} = 0, \tag{1.1}$$

where **v** is velocity and ρ is the density of a mass element $dm = \rho\, dV$. Choosing a dimensionless constant β in (1.1), the field **B** obtains the dimension of a magnetic induction field. Depending on the definition of the field **B**, different values for the dimensionless constant β of order unity have been introduced in the past (see ref. [7, p.7] for a discussion of this point). Moreover, alternative choices for the dimension of the field **B** are mathematically possible, leading to other dimensions for β. It is noticed that Gaussian units are used throughout this paper.

Since $\nabla.\mathbf{B} = 0$, the field **B** can be derived from a gravitomagnetic vector potential **A** ($\mathbf{B} = \nabla\times\mathbf{A}$). The field **B** can be derived in a similar way as in the corresponding electromagnetic case (see, e.g., Landau and Lifshitz [9, § 43 and § 44]). For a massive rotating sphere with angular momentum **S** the following expression satisfies to (1.1)

$$\mathbf{A} = \tfrac{1}{2}\beta c^{-1}G^{1/2}\,\mathbf{S}\times\nabla\left(1/R\right) = -\tfrac{1}{2}\beta c^{-1}G^{1/2}R^{-3}\,\mathbf{S}\times\mathbf{R}. \tag{1.2}$$

Here **R** is the position vector from the centre of the sphere to the field point *F*, where the vector potential **A** is measured (*R* is the corresponding scalar value of **R**). This expression applies when *R* is much larger than the radius r_0 of the sphere, but it displays the flaw of a singularity at $R = 0$. Special attention will be paid in this work to the vector potential **A** inside the sphere. Moreover, the case $R \approx r_0$ will be investigated.

The angular momentum **S** of the sphere with total mass *m* in (1.2) is given by

$$\mathbf{S} = I\boldsymbol{\omega}, \quad \text{and} \quad S = I\omega = \tfrac{2}{5}\,f_s m r_0^2\,\omega, \tag{1.3}$$

where $\boldsymbol{\omega}$ is the angular momentum vector ($\omega = 2\pi\nu$ is the angular velocity of the sphere and ν is its rotational frequency), *I* is the moment of inertia of the sphere and f_s is a dimensionless factor depending on the homogeneity of the mass density ρ of the sphere. For a homogeneous mass density $f_s = 1$, but when the mass density is greater near the centre of the sphere f_s will be less than unity value. In this work the former case will be considered.

The expression for **A** in (1.2) can be rewritten in terms of the gravitomagnetic dipole moment **M** defined by

$$\mathbf{M} = -\tfrac{1}{2}\beta c^{-1}G^{1/2}\,\mathbf{S}. \tag{1.4}$$

Insertion of (1.4) into (1.2) then yields

$$\mathbf{A} = \frac{\mathbf{M}\times\mathbf{R}}{R^3}. \tag{1.5}$$

For $R \geq r_0$ this expression represents the gravitomagnetic vector potential **A** of an ideal dipole, located in the centre of the sphere. Combining (1.3) and (1.4) leads to the relations

$$\mathbf{M} = -\tfrac{1}{5}\beta c^{-1}G^{1/2}m r_0^2\,\boldsymbol{\omega}, \quad \text{or} \quad M = -\tfrac{1}{5}\beta c^{-1}G^{1/2}m\omega r_0^2. \tag{1.6}$$

Combination of (1.5) and (1.6) yields the following components for the vector potential **A** expressed in spherical coordinates (R, θ and φ)

$$A_R = 0, \quad A_\theta = 0 \quad \text{and} \quad A_\varphi = \frac{M\sin\theta}{R^2} = -\frac{\beta G^{1/2}m\omega r_0^2\sin\theta}{5cR^2}, \tag{1.7}$$

where θ is the angle between the directions of the vectors **S** and **R**.

Subsequently, the components of the gravitomagnetic field **B** in spherical coordinates can be calculated from $\mathbf{B} = \nabla\times\mathbf{A}$

$$B_R = \frac{1}{R\sin\theta}\frac{\partial}{\partial\theta}\left(\sin\theta A_\varphi\right), \quad B_\theta = -\frac{1}{R}\frac{\partial}{\partial R}\left(RA_\varphi\right) \quad \text{and} \quad B_\varphi = 0. \tag{1.8}$$

Insertion of (1.7) into (1.8) leads to the following expressions for B_R and B_θ

$$B_R = \frac{2M\cos\theta}{R^3} = -\frac{2\beta G^{1/2}m\omega r_0^2\cos\theta}{5cR^3}, \tag{1.9}$$

$$B_\theta = \frac{M \sin\theta}{R^3} = -\frac{\beta G^{1/2} m \omega r_0^2 \sin\theta}{5cR^3}. \tag{1.10}$$

By combining (1.9) and (1.10) the following vector expression for the field **B** follows

$$\mathbf{B} = \left(\frac{3\mathbf{M}\cdot\mathbf{R}}{R^5}\mathbf{R} - \frac{\mathbf{M}}{R^3} \right). \tag{1.11}$$

Note that this equation is completely analogous to the corresponding electromagnetic relation. At large distance R from the centre of the sphere, the gravitomagnetic field **B** is adequately described by the dipole field of (1.11). In the vicinity of the sphere, however, deviations may occur. The dipole model is not generally valid within the sphere and fails, when R approaches to zero value. Since observational tests are often carried out near or at the surface of the sphere, special attention is paid to the region $R \approx r_0$ in this study.

A first measurement of Earth's gravitomagnetic field **B** has been performed by Ciufolini *et al.* [10–13] by analysing the precession of the orbits with $R \approx 1.9r_0$ of two artificial satellites: LAGEOS (laser geodynamics satellite) and LAGEOS 2. The satellites can be regarded as gyroscopes with an angular momentum $\mathbf{S}_{\rm orbit}$, which is subjected to Earth's gravitomagnetic field **B** (and its gravity field). The precession of $\mathbf{S}_{\rm orbit}$ around field **B** is called the Lense-Thirring precession. Another spacecraft, Gravity Probe B, equipped with a set of four spherical gyroscopes, was launched in a polar orbit with $R \approx 1.1r_0$ around the Earth in 2004. Last year, the observed precessions of the gyroscopes, depending on the gravitomagnetic field **B** were published by Everitt *et al.* [14]. A comparison of observed and theoretical results of both missions has been given by Biemond [15]. In addition, Bosi *et al.* [16] are planning an underground ring-laser experiment for the observation of Earth's gravitomagnetic field **B**. Using a tri-axial laser detector, they will try to separate the gravitomagnetic precession rate and the geodetic precession rate of the light probe from Earth's rotation rate.

It has previously been proposed [5–7, 15, 17–19], that the gravitomagnetic field **B** = **B**(gm) generated by rotating mass and the electromagnetic field **B**(em) due to moving charge may be equivalent. Application of this special interpretation of the gravito-magnetic field results in the deduction of four new *gravitomagnetic* precession frequencies, which have been identified with observed low frequency QPOs [18] for pulsars and black holes. Predictions of the proposed model were compared with observed low frequency QPOs of the pulsars SAX J1808.4−3658, XTE J1807−294, IGR J00291+5934 and SGR 1806−20. The results seem to be compatible with the presented model. Moreover, similar results have been obtained for the stellar black hole XTE J1550−564 and the supermassive black hole Sgr A* [19]. The proposed interpretation is in contradiction with the results reported from Gravity Probe B and LAGEOS satellites.

Starting from a rotating circular torus with homogeneous mass density, truncated series expansions for the φ-component A_φ of the vector potential **A** of a rotating sphere have recently been calculated [15] for the whole interval from $R = 0$ to $R \to \infty$. In section 2 of this work the latter result is compared with the proposed, internal (i.e., $0 \le R \le r_0$) vector potential $\mathbf{A}_{\rm int}$ for a sphere. In section 3 a quantitative derivation is given for the internal axial gravitomagnetic field $\mathbf{B}_{\rm int,\,ax}$. Two limiting cases ($R \to 0$ and $R = r_0$) follow from this new formula for $\mathbf{B}_{\rm int,\,ax}$. In section 4 a general expression for the internal gravitomagnetic field $\mathbf{B}_{\rm int}$ is proposed and checked. Application of Stokes' theorem to (1.1a) in section 5, leads to an alternative calculation of component B_θ of the gravitomagnetic field **B** for $R = r_0$. In section 6 the electromagnetic vector potential **A**(em) and electromagnetic field **B**(em) are given and discussed. In section 7 the properties of the gravitomagnetic field **B** at different values of R are discussed. Finally, in section 8 a comparison with observations is given and conclusions are drawn.

2. THE GRAVITOMAGNETIC VECTOR POTENTIAL A

The external vector potential **A** given in (1.5) applies to the range $R \geq r_0$. For the interval $0 \leq R \leq r_0$ the following important vector potential **A** of the sphere, $\mathbf{A}_{\text{int}}$, will firstly be postulated

$$\mathbf{A}_{\text{int}} = \frac{\mathbf{M}\times\mathbf{R}}{r_0^3}\left(\frac{5}{2}-\frac{3}{2}\frac{R^2}{r_0^2}\right). \tag{2.1}$$

This relation can, however, be checked for several limiting cases. As a simple example, for $R = r_0$ (2.1) reduces to (1.5), representing the external ($R \geq r_0$), gravitomagnetic vector potential of an ideal dipole.

Utilizing (1.6), the component $A_{\varphi,\,\text{int}}$ can be found from (2.1) (compare with (1.7))

$$A_{\varphi,\,\text{int}} = \frac{M\sin\theta}{r_0^2}\left(\frac{5}{2}\frac{R}{r_0}-\frac{3}{2}\frac{R^3}{r_0^3}\right) = -\frac{\beta G^{1/2} m\,\omega \sin\theta}{c}\left(\frac{1}{2}\frac{R}{r_0}-\frac{3}{10}\frac{R^3}{r_0^3}\right), \tag{2.2}$$

whereas the components $A_{R,\,\text{int}}$ and $A_{\theta,\,\text{int}}$ are zero. For small values of R the equatorial component $A_{\varphi,\,\text{int}}$ of (2.2) (i.e., $\theta = 90°$), denoted by $A_{\varphi,\,\text{int, eq}}$, reduces to

$$A_{\varphi,\,\text{int, eq}} = \frac{5MR}{2r_0^3} = -\frac{\beta G^{1/2} m\,\omega R}{2cr_0}. \tag{2.3}$$

This linear relationship between $A_{\varphi,\,\text{int, eq}}$ and R can also be derived by a more simple calculation [15]. Note that $A_{\varphi,\,\text{int, eq}}$ reduces to zero value in the limiting case $R \to 0$. The validity of (2.2) in the equatorial plane (i.e., $\theta = 90°$) will further be discussed below.

In order to find a rigorous derivation of the component A_φ of the sphere for the range $0 \leq R \leq \infty$, we now first calculate the component $A_{\varphi'}$ for a circular torus containing a total mass $dm = \rho\, dV$ (ρ is the homogeneous mass density of the torus). The derivation of $A_{\varphi'}$ follows from a method given by Jackson [20]. As an example, a torus lying in an x'-y' plane at distance s from the origin O' is chosen, as shown in figure 1. The x'-y' plane is parallel to the x-y plane through the centre O of the sphere. A radius vector $\mathbf{R}'$ from O' to a field point F is fixed by the spherical coordinates R', θ' and $\varphi' = 0$. At field point F, the mass current $dm/dt = dm\,\nu$ (ν is the frequency of the mass current) in the torus generates the following azimuthal component of the vector potential **A** in the y direction, i.e. $A_{\varphi'}(R',\theta')$

$$A_{\varphi'}(R',\theta') = \frac{-8\beta G^{1/2} dm\,\nu s}{c(s^2+R'^2+2sR'\sin\theta')^{1/2}}\left\{\frac{(1-\tfrac{1}{2}k^2)K(k)-E(k)}{k^2}\right\}, \tag{2.4}$$

where $K(k)$ and $E(k)$ are complete elliptic integrals of the first kind and second kind, respectively. See for the properties of these integrals, e.g., [21, § 2.57, § 8.11–§ 8.12]. The modulus k of the elliptic integrals is given by

$$k^2 = \frac{4sR'\sin\theta'}{s^2+R'^2+2sR'\sin\theta'}. \tag{2.5}$$

A number of limiting cases for $A_{\varphi'}(R',\theta')$ can be distinguished. When $\theta' \approx 0$, $R' >> s$, or $s >> R'$, k^2 is small. Then, $A_{\varphi'}(R',\theta')$ of (2.4) reduces to relative simple expressions. For $k = 1$

$K(k)$ and $A_{\varphi'}(R', \theta')$ become infinite. We will now first consider the limiting case $\theta' \approx 0$. Subsequently, an example of $R' >> s$, or $R' \to \infty$ with F in the x-y plane (i.e., the equatorial plane) will be considered.

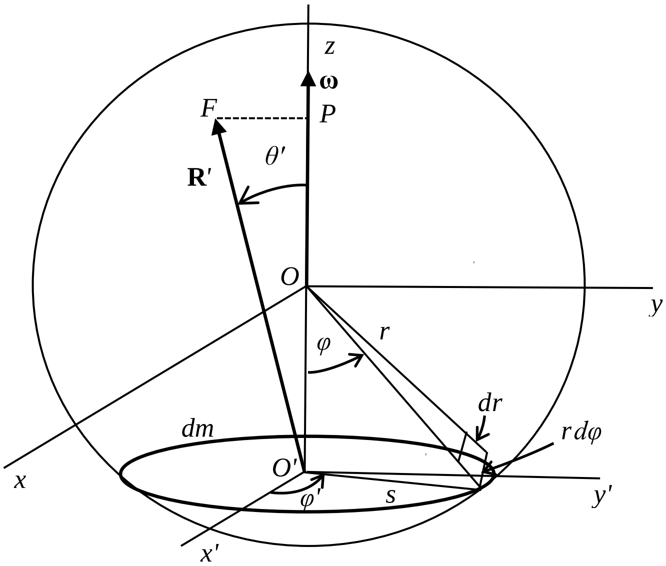

Figure 1. Spherical coordinates R', θ' and $\varphi' = 0$ of a field point F relative to the origin O'. A point mass δm in a torus is located in the x'-y' plane at coordinates s and $\varphi' = \varphi'$. The total mass dm of the torus is given by $\sum \delta m = dm = \rho dV = 2\pi\rho s r d\varphi dr$. The angular velocity vector of the sphere is given by $\boldsymbol{\omega}$. The distance $OP = R$ denotes a position below or at the pole of the sphere.

In the limiting case $\theta' \approx 0$, the value of k^2 is small and the expression between parentheses in (2.4), denoted by $F(k)$, reduces to

$$F(k) = \frac{(1 - \tfrac{1}{2}k^2)K(k) - E(k)}{k^2} \approx \frac{\pi k^2}{32}. \tag{2.6}$$

Combination of (2.4)–(2.6) then yields for $A_{\varphi'}(R', \theta')$ (compare with Jackson [20])

$$A_{\varphi'}(R', \theta') = \frac{-\beta G^{1/2} dm\, \omega\, s^2 R' \sin\theta'}{2c(s^2 + R'^2 + 2sR' \sin\theta')^{3/2}}, \tag{2.7}$$

where the relation $\omega = 2\pi\nu$ has been inserted. When a field point P is chosen in the vicinity of the rotation axis, the angle θ' and $A_{\varphi'}(R', \theta')$ approach to zero value. According to (1.8a), however, the gravitomagnetic field $B_{R'}(R', \theta')$ need not to be zero (in section 3 the latter field is calculated).

When values of $\theta' >> 0$ occur, the approximate value of $F(k)$ in (2.6) is no longer valid and a series expansion of $F(k)$ in terms of k^2 is possible. Such an evaluation up to the terms in k^{14}, has recently been performed [15] for field points F, lying in the equatorial plane of the sphere (i.e., the x-y plane in figure 1). In this calculation the parameters R', θ' and s occurring in (2.4) and (2.5), are replaced by the coordinates R, r and φ, where

$$R = R' \sin\theta', \quad O'O = r\cos\varphi, \quad R'^2 = r^2 \cos^2\varphi + R^2 \quad \text{and} \quad s = r \sin\varphi. \tag{2.8}$$

In addition, the following relations are used

$$dm = 2\pi\rho \sin\varphi \, d\varphi \, r^2 dr \quad \text{and} \quad m = {}^4\!/_3 \, \pi \rho r_0^3. \tag{2.9}$$

The obtained double integral depending on φ and r is first integrated over φ from $\varphi = 0$ to $\varphi = \pi$. Subsequently, the remaining integral is integrated over r from $r = 0$ to $r = r_0$. The following complicated result for the equatorial component A_φ, denoted by $A_{\varphi,\text{eq}}$, of the sphere is then obtained [15]

$$\begin{aligned} A_{\varphi,\text{eq}} = \frac{-\beta G^{1/2} m\omega R}{c r_0} \Bigg[& \left\{ \frac{-\frac{5}{2} r_0^2 - 2 r_0 R}{(r_0+R)^2} + 3 - 6\frac{R}{r_0} + 6\frac{R^2}{r_0^2} \ln\left(\frac{r_0+R}{R}\right) \right\} \\ & + \left\{ \frac{-12 r_0^3 R - \frac{115}{4} r_0^2 R^2 - 25 r_0 R^3 - \frac{15}{2} R^4}{(r_0+R)^4} + 15\frac{R}{r_0} - 15\frac{R^2}{r_0^2} \ln\left(\frac{r_0+R}{R}\right) \right\} \\ & + \left\{ \frac{-\frac{441}{20} r_0^5 R^2 - \frac{783}{10} r_0^4 R^3 - \frac{513}{4} r_0^3 R^4 - 111 r_0^2 R^5 - \frac{99}{2} r_0 R^6 - 9R^7}{r_0 (r_0+R)^6} + 9\frac{R^2}{r_0^2} \ln\left(\frac{r_0+R}{R}\right) \right\} \\ & + \left\{ \frac{7}{2} \frac{R^2}{r_0^2} \frac{r_0^8}{(r_0+R)^8} \right\} + \left\{ \frac{R^2}{r_0^2} \frac{r_0^{10} + 10 r_0^9 R}{(r_0+R)^{10}} \right\} + \left\{ \frac{9}{20} \frac{R^2}{r_0^2} \frac{r_0^{12} + 12 r_0^{11} R + 66 r_0^{10} R^2}{(r_0+R)^{12}} \right\} \\ & + \left\{ \frac{1}{4} \frac{R^2}{r_0^2} \frac{r_0^{14} + 14 r_0^{13} R + 91 r_0^{12} R^2 + 364 r_0^{11} R^3}{(r_0+R)^{14}} \right\} \Bigg]. \end{aligned} \tag{2.10}$$

This results applies to the whole interval from $R = 0$ to $R \to \infty$. For very large values of R the r. h. s. of $A_{\varphi,\text{eq}}$ in (2.10) reduces to the external φ-component $A_{\varphi,\text{ext,eq}}$

$$A_{\varphi,\text{ext,eq}} = -\frac{\beta G^{1/2} m \omega r_0^2}{5 c R^2} = \frac{M}{R^2}. \tag{2.11}$$

This relation coincides with the ideal dipole result of (1.7c) for $\theta = 90°$. It is noticed, that apart from the term in $(r_0/R)^2$ in (2.11) the series expansion of $A_{\varphi,\text{ext,eq}}$ in (2.10) also produces terms in $(R/r_0)^2$, R/r_0, real numbers, r_0/R, $(r_0/R)^2$, $(r_0/R)^3$, $(r_0/R)^4$, $(r_0/R)^6$, $(r_0/R)^7$ and $(r_0/R)^8$, but their sums all cancel (higher order terms than $(r_0/R)^8$ have not been calculated). Only the term in $(r_0/R)^2$ survives in the performed calculation.

In addition, the r. h. s. of $A_{\varphi,\text{eq}}$ in (2.10) for the interval $0 \le R \le r_0$ can be rewritten as (terms up to $(R/r_0)^7$ have been calculated)

$$A_{\varphi,\text{int,eq}} = \frac{-\beta G^{1/2} m\omega}{c} \left(\frac{1}{2}\frac{R}{r_0} - \frac{11}{10}\frac{R^3}{r_0^3} \right). \tag{2.12}$$

Apart from the terms in R/r_0 and $(R/r_0)^3$, all terms of the truncated series expansion, like terms in $(R/r_0)^2$, $(R/r_0)^4$, $(R/r_0)^5$, $(R/r_0)^6$ and $(R/r_0)^7$ reduce to zero value. Moreover, the coefficient 11/10 of the surviving term in $(R/r_0)^3$ will decrease, when terms higher than seventh order in R/r_0 are taken into account in an extended calculation of (2.10).

The postulated formula for A_φ in (2.2) reduces for $\theta = 90°$ to the following expression for $A_{\varphi,\text{int,eq}}$ (see also comment to (2.3))

$$A_{\varphi,\text{int,eq}} = \frac{-\beta G^{1/2} m\omega}{c} \left(\frac{1}{2}\frac{R}{r_0} - \frac{3}{10}\frac{R^3}{r_0^3} \right). \tag{2.13}$$

Table 1. The terms *T1* through *T7* of $A_{\varphi,\mathrm{eq}}$ from the r. h. s. of (2.10) are given, expressed in units of $-\beta c^{-1}G^{½}m\omega$, for different values of R, expressed in units of r_0. In addition, the sum of the seven contributions to $A_{\varphi,\mathrm{eq}}$, S, again in units of $-\beta c^{-1}G^{½}m\omega$, is added. Moreover, the values of $A_{\varphi,\mathrm{int,eq}}$ from (2.13), E (educated guess), and $A_{\varphi,\mathrm{ext,eq}}$ from (2.11), D (ideal dipole model), in units of $-\beta c^{-1}G^{½}m\omega$, are also given for values of $0 \le R \le r_0$ and $R \ge r_0$, respectively. The ratio S/D in percent is added, too. See also text.

Term number	$R = 0$	$R = 0.1r_0$	$R = 0.2r_0$	$R = 0.3r_0$	$R = 0.4r_0$	$R = 0.5r_0$
1	0	+0.0312469	+0.0432267	+0.0472507	+0.0475916	+0.0461814
2	0	+0.0106746	+0.0221416	+0.0289268	+0.0319998	+0.0326946
3	0	+0.0039251	+0.0116314	+0.0178846	+0.0215995	+0.0231816
4	0	+0.0016328	+0.0065119	+0.0115847	+0.0151783	+0.0170706
5	0	+0.0007711	+0.0387613	+0.0078341	+0.0110629	+0.0130061
6	0	+0.0004101	+0.0243873	+0.0054966	+0.0083107	+0.0101881
7	0	+0.0002419	+0.0161256	+0.0039804	+0.0064011	+0.0081623
S	0	+0.0475115	+0.0865397	+0.1153536	+0.1333668	+0.1415765
E	0	+0.0497	+0.0976	+0.1419	+0.1808	+0.2125

Term number	$R = 0.6r_0$	$R = 0.7r_0$	$R = 0.8r_0$	$R = 0.9r_0$	$R = r_0$	$R = 1.1r_0$
1	+0.0439672	+0.0414333	+0.0388319	+0.0362936	+0.0338831	+0.0316289
2	+0.0319887	+0.0305148	+0.0286632	+0.0266683	+0.0246673	+0.0227371
3	+0.0232930	+0.0224948	+0.0211883	+0.0196387	+0.0180121	+0.0164081
4	+0.0176020	+0.0172096	+0.0162614	+0.0150233	+0.0136719	+0.0123166
5	+0.0137516	+0.0136112	+0.0129059	+0.0118903	+0.0107422	+0.0095756
6	+0.0110365	+0.0110579	+0.0105239	+0.0096726	+0.0086792	+0.0076589
7	+0.0090516	+0.0091792	+0.0087701	+0.0080442	+0.0071716	+0.0062674
S	+0.1421401	+0.1374703	+0.1296533	+0.1202518	+0.1103271	+0.1005433
D					+0.2	+0.1652893
E	+0.2352	+0.2471	+0.2464	+0.2313	+0.2	
S/D (%)					55.16	60.83

Term number	$R = 1.2r_0$	$R = 1.3r_0$	$R = 1.4r_0$	$R = 1.5r_0$	$R = 1.6r_0$	$R = 1.7r_0$
1	+0.0295400	+0.0276142	+0.0258439	+0.0242189	+0.0227277	+0.0213588
2	+0.0209182	+0.0192289	+0.0176746	+0.0162528	+0.0149571	+0.0137787
3	+0.0148825	+0.0134640	+0.0121641	+0.0109843	+0.0099202	+0.0089644
4	+0.0110212	+0.0098192	+0.0087249	+0.0077414	+0.0068650	+0.0060884
5	+0.0084579	+0.0074247	+0.0064918	+0.0056623	+0.0049326	+0.0042952
6	+0.0066805	+0.0057809	+0.0049757	+0.0042680	+0.0036536	+0.0031248
7	+0.0054007	+0.0046085	+0.0039061	+0.0032960	+0.0027736	+0.0023305
S	+0.0912805	+0.0827297	+0.0749623	+0.0679783	+0.0617383	+0.0561829
D	+0.1388889	+0.1183432	+0.1020408	+0.0888889	+0.078125	+0.0692042
S/D (%)	65.72	69.91	73.46	76.48	79.03	81.18

Term number	$R = 1.8r_0$	$R = 1.9r_0$	$R = 2.0r_0$	$R = 2.5r_0$	$R = 3.0r_0$	$R = 10r_0$
1	+0.0201015	+0.0189453	+0.0178807	+0.0136599	+0.0107457	+0.0015747
2	+0.0127084	+0.0117364	+0.0108537	+0.0074995	+0.0053622	+0.0003321
3	+0.0081080	+0.0073417	+0.0066565	+0.0041702	+0.0027153	+0.0000717
4	+0.0054028	+0.0047989	+0.0042676	+0.0024285	+0.0014420	+0.0000163
5	+0.0037410	+0.0032607	+0.0028451	+0.0014727	+0.0007982	+0.0000039
6	+0.0026721	+0.0022861	+0.0019577	+0.0009228	+0.0004570	+0.0000010
7	+0.0019572	+0.0016440	+0.0013820	+0.0005938	+0.0002688	+0.0000002
S	+0.0512453	+0.0468582	+0.0429577	+0.0289126	+0.0206161	+0.0019838
D	+0.0617284	+0.0554017	+0.05	+0.032	+0.0222222	+0.002
S/D (%)	83.02	84.58	85.92	90.35	92.77	99.19

Compared to (2.10), this choice for $A_{\varphi,\text{int,eq}}$ implies that all terms $(R/r_0)^n$ with $n > 8$ in (2.10) are supposed to be zero. Moreover, the additional contributions to the term in $(R/r_0)^3$ have to converge to a total term $3/10(R/r_0)^3$, instead of the term $11/10(R/r_0)^3$ obtained in (2.12).

The right hand side of (2.10) contains seven terms between parentheses, denoted by *T1* up to *T7*. For increasing values of R in the interval $0 \le R \le 10r_0$ the separate values of these terms have been given in table 1, expressed in units of $-\beta c^{-1}G^{½}m\omega$. Moreover, the sum S of these seven terms has also been added. In addition, the values of the vector potential $A_{\varphi,\text{int,eq}}$ from (2.13), denoted by E (educated guess), and again expressed in units of $-\beta c^{-1}G^{½}m\omega$, have been given for the interval $0 \le R \le r_0$. Finally, the values of $A_{\varphi,\text{ext,eq}}$ from (2.11) for an ideal dipole, denoted by D and given in units of $-\beta c^{-1}G^{½}m\omega$ for the interval $r_0 \le R \le 10r_0$ have been included. The absolute value of the ratio S/D in percent is also added to table 1. It appears that the values of D are always more negative than those of S. For values of $R \ge 10r_0$ both values coincide within 0.8%.

In figure 2 the terms *T1*, *T2*, *T3*, *T5*, *T7*, the sum S, and the vector potential E have been plotted against increasing values of R. The *T1* curve accurately describes the behavior of the vector potential $A_{\varphi,\text{eq}}$ for the limiting cases $R \to 0$ and $R \to \infty$. It can be seen from figure 2, that the maximum values for *T1* up to *T7* shift to higher values of R. The S versus R curve illustrates the more accurate overall behaviour of A_φ, but is still a rough approximation. The result for S would improve when more terms in the series expansion of (2.10) would have taken into account, but their calculation is too cumbersome. The S versus R curve can be compared with E versus R curve from (2.13) for the interval $0 \le R \le r_0$ Calculation from (2.13) shows, that maximum value of the E occurs for $R = ⅓(5)^{½}r_0 = 0.7454r_0$. The D versus R curve from (2.11) for the interval $r_0 \le R \le 2r_0$ has also been given. For $R = r_0$ the functions E and D are equal and continuous ($\partial A_{\varphi,\text{eq}}/\partial R = -2M/R^3$). The area between the S curve one side and the E and D curves on the other side may reflect our uncertainty.

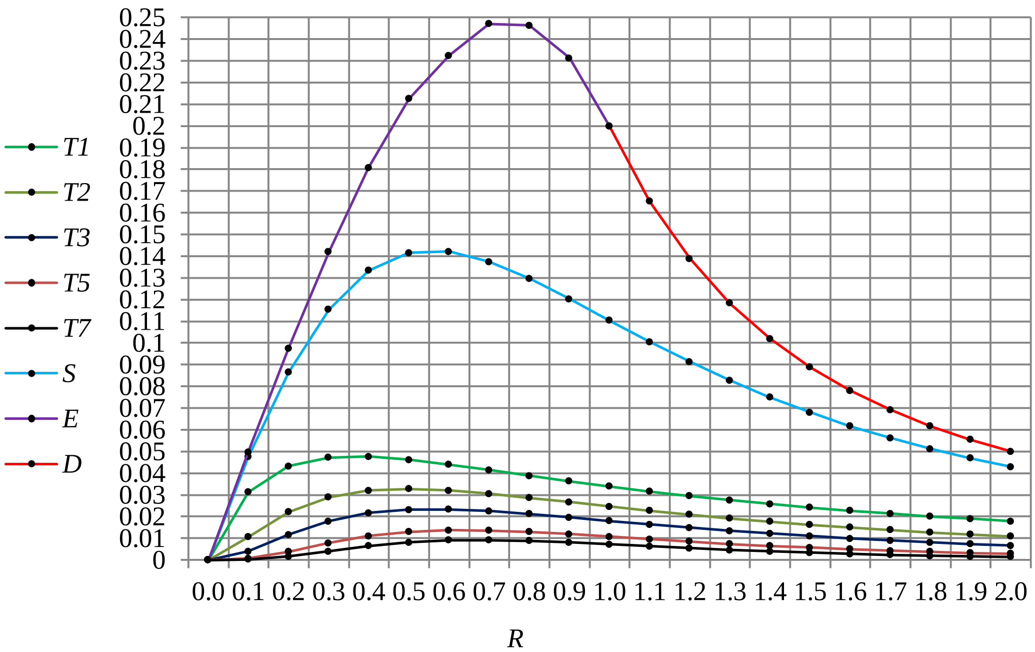

Figure 2. Values of the terms *T1*, *T2*, *T3*, *T5*, *T7* and the sum S of the terms *T1* through *T7* of $A_{\varphi,\text{eq}}$ from (2.10), all expressed in units of $-\beta c^{-1}G^{½}m\omega$, have been plotted against increasing values of R, in units of r_0. In addition, the vector potential E from (2.13) and the ideal dipole value D from (2.11) have been plotted in the same way. The values of E are given for the interval $0 \le R \le r_0$, whereas those for D are shown for the interval $r_0 \le R \le 2r_0$. See also text.

3. THE INTERNAL AXIAL GRAVITOMAGNETIC FIELD $\mathbf{B}_{\mathrm{int,ax}}$ OF A SPHERE

Starting from the potential $A_{\varphi'}(R', \theta')$ of (2.7), the internal (i.e., $0 \geq R \geq r_0$) gravitomagnetic field at a field point F, located on the rotation axis, will be calculated in this section. Application of (1.8a) to this approximated (i.e., $\theta' \approx 0$) expression yields the radial component $B_{R'}(R',\theta')$ for the gravitomagnetic field, due to a torus with radius s and mass dm

$$B_{R'}(R',\theta') = \frac{-\beta G^{1/2} dm\,\omega s^2\left(2s^2 + 2R'^2 + sR'\sin\theta'\right)\cos\theta'}{2c(s^2 + R'^2 + 2sR'\sin\theta')^{5/2}}. \tag{3.1}$$

When the angle θ' in (3.1) reduces to zero, the field point F shifts to the rotation axis of the sphere, or z-axis (see figure 3a). Eq. (3.1) then simplifies to

$$B_{R'}(s,R') = \frac{-\beta G^{1/2} dm\,\omega s^2}{c(s^2 + R'^2)^{3/2}}. \tag{3.2}$$

Note that the field $B_{R'}(s,R')$ has always a negative sign for the choice $\beta = +1$. The mass of the torus dm in (3.2) can be written as

$$dm = \rho dV = 2\pi\rho s ds|dR'|. \tag{3.3}$$

Substitution of (3.3) and (2.9b) into (3.2) yields

$$B_{R'}(s,R') = \frac{-3\beta G^{1/2} m\omega s^3 ds|dR'|}{2cr_0^3(s^2 + R'^2)^{3/2}}. \tag{3.4}$$

When $B_{R'}(s,R')$ is integrated over s from $s = 0$ to $s = s_0$, one obtains

$$B_{R'}(R') = \frac{-3\beta G^{1/2} m\omega}{2cr_0^3}\left\{(s_0^2 + R'^2)^{1/2} + \frac{R'^2}{(s_0^2 + R'^2)^{1/2}} - 2R'\right\}|dR'|. \tag{3.5}$$

$B_{R'}(R')$ represents the field at distance R' from a disk with radius s_0 and a thickness of $|dR'|$, acting at the field point F located on the rotation axis (see figure 3a and 3b).

We now first calculate the contribution to the radial field, denoted by $B_R(\mathrm{low})$, from the lower part of the sphere (i.e., the part of the sphere below the plane through point F and perpendicular to the direction of the angular momentum vector $\boldsymbol{\omega}$ (see figure 3a)). In that case, (3.5) can further be evaluated by utilizing the following relations

$$s_0 = r_0\sin\varphi, \quad R' = r_0\cos\varphi + R \quad \text{and} \quad |dR'| = r_0\sin\varphi\, d\varphi, \tag{3.6}$$

where the distance OF is replaced by R ($0 \geq R \geq r_0$, see figure 3a). Insertion of (3.6) into (3.5), followed by integration over φ from $\varphi = 0$ to $\varphi = \varphi_0$ ($\cos\varphi_0 = -R/r_0$) yields for $B_{R,\mathrm{low}}$

$$B_{R,\mathrm{low}} = \frac{\beta G^{1/2} m\omega}{cr_0^3}\left\{\frac{(r_0 - R)(r_0 + R)^3}{R^2} + \frac{(r_0^2 - R^2)^{3/2}}{2R} + \frac{(r_0^2 - R^2)^{5/2}}{5R^3} - \frac{(r_0 + R)^5}{5R^3} + \frac{3(r_0 + R)^2}{2}\right\}. \tag{3.7}$$

In the integration over φ the quantity R has been considered as a constant parameter. The field $B_{R,\mathrm{low}}$, acting at point F, represents the field from the lower part of the sphere.

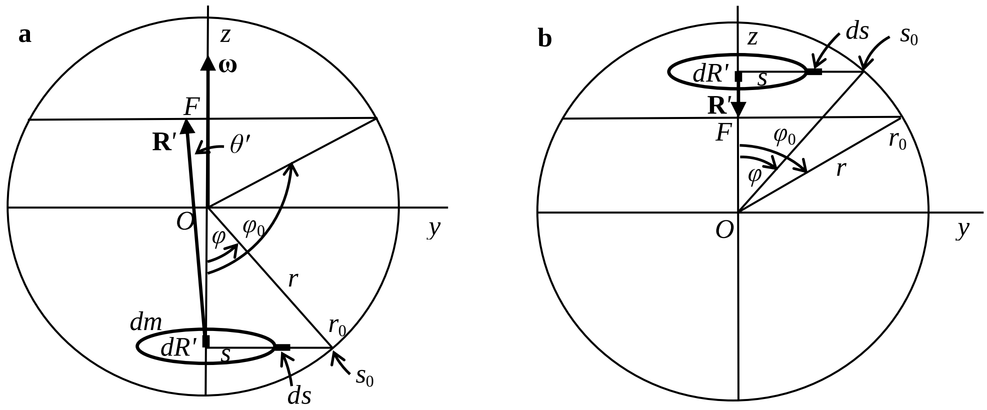

Figure 3. Calculation of the axial gravitomagnetic field $B_{R,\,\mathrm{int,\,ax}}$ at field point F, located on the rotation axis. The calculation starts with the gravitomagnetic field $B_{R'}(R',\theta')$ of (3.1) for a torus with radius s and mass dm at a position with coordinates R' and θ' near the rotation axis (see figure 3a). Subsequently, the field $B_{R'}(R')$ of (3.5) at point F ($OF = R$) at distance R' from a disk with radius s_0 and a thickness of $|dR'|$, is calculated. Finally, by integrating over φ from $\varphi = 0$ to $\varphi = \varphi_0$ the field $B_{R,\,\mathrm{low}}$ of (3.7) is obtained, representing the total field of the sphere minus the upper part above the field point F (see figure 3a). Likewise, using figure 3b, the field $B_{R,\,\mathrm{high}}$ of (3.9) of the upper part can be found. The sum $B_{R,\,\mathrm{int,\,ax}} = B_{R,\,\mathrm{low}} + B_{R,\,\mathrm{high}}$ is given by (3.10a).

The part of the sphere above the plane through point F and perpendicular the direction of rotation axis or z-axis (see figure 3b) also contribute to the radial field and will be denoted by $B_{R,\,\mathrm{high}}$. The distance OF is again replaced by R. In order to calculate $B_{R,\,\mathrm{high}}$, expression (3.5) can be used as starting point. This equation can be evaluated by utilizing the relations

$$s_0 = r_0 \sin\varphi, \quad R' = r_0\cos\varphi - R \quad \text{and} \quad |dR'| = r_0 \sin\varphi\, d\varphi. \tag{3.8}$$

Insertion of (3.8) into (3.5), followed by integration over φ from $\varphi = 0$ to $\varphi = \varphi_0$ ($\cos\varphi_0 = R/r_0$) yields the field $B_{R,\,\mathrm{high}}$

$$B_{R,\,\mathrm{high}} = \frac{\beta G^{1/2} m\omega}{c r_0^3}\left\{\frac{(r_0+R)(r_0-R)^3}{R^2} - \frac{(r_0^2-R^2)^{3/2}}{2R} - \frac{(r_0^2-R^2)^{5/2}}{5R^3} + \frac{(r_0-R)^5}{5R^3} + \frac{3(r_0-R)^2}{2}\right\}. \tag{3.9}$$

The total radial field of the sphere $B_{R,\,\mathrm{int,\,ax}}$, acting at field point F on the rotation axis, is given by the sum $B_{R,\,\mathrm{int,\,ax}} = B_{R,\,\mathrm{low}} + B_{R,\,\mathrm{high}}$ from (3.7) and (3.9), respectively. Calculation yields for $B_{R,\,\mathrm{int,\,ax}}$, and for the internal axial gravitomagnetic field $\mathbf{B}_{\mathrm{int,\,ax}}$

$$B_{R,\,\mathrm{int,\,ax}} = -\frac{\beta G^{1/2} m\omega}{c r_0}\left(1 - \frac{3}{5}\frac{R^2}{r_0^2}\right), \quad \text{or} \quad \mathbf{B}_{\mathrm{int,ax}} = \frac{5\mathbf{M}}{r_0^3}\left(1 - \frac{3}{5}\frac{R^2}{r_0^2}\right). \tag{3.10}$$

To my knowledge, this exact expression for the internal, axial gravitomagnetic field $\mathbf{B}_{\mathrm{int,\,ax}}$ has been derived here for the first time.

Two limiting values for $\mathbf{B}_{\mathrm{int,\,ax}}$ follow directly from (3.10): firstly, the field in the centre of the sphere, $\mathbf{B}_{\mathrm{c}}$, and secondly, the field at the poles of the sphere, $\mathbf{B}_{\mathrm{p}}$

$$\mathbf{B}_{\mathrm{c}} = -\frac{\beta G^{1/2} m\boldsymbol{\omega}}{c r_0} = \frac{5\mathbf{M}}{r_0^3} \quad \text{and} \quad \mathbf{B}_{\mathrm{p}} = -\frac{2\beta G^{1/2} m\boldsymbol{\omega}}{5 c r_0} = \frac{2\mathbf{M}}{r_0^3}. \tag{3.11}$$

The latter results can be found more easily [15]. Note that the polar gravitomagnetic field $\mathbf{B}_p$ appears to coincide with the field from the ideal dipole approximation for $R = r_0$ (compare with (1.9)). Moreover, the result for $\mathbf{B}_c$ of (3.11) shows no singularity at $R = 0$, whereas the ideal dipole model of (1.9) and (1.10) displays such a flaw.

4. THE INTERNAL GRAVITOMAGNETIC FIELD $\mathbf{B}_{int}$ OF A SPHERE

In order to find the general expression for the internal gravitomagnetic field $\mathbf{B}_{int}$ of a sphere, we start from the postulated expression for the gravitomagnetic vector potential $\mathbf{A}_{int}$ of (2.1) (see (2.2) for $A_{\varphi,int}$). Application of (1.8) to (2.2) yields for $B_{R,int}$ and $B_{\theta,int}$, respectively

$$B_{R,\,int} = \frac{M\cos\theta}{r_0^3}\left(5 - \frac{3R^2}{r_0^2}\right), \tag{4.1}$$

$$B_{\theta,\,int} = \frac{M\sin\theta}{r_0^3}\left(-5 + \frac{6R^2}{r_0^2}\right). \tag{4.2}$$

In addition, from $A_{R,int} = A_{\theta,int} = 0$ follows that $B_{\varphi,int} = 0$. It is noticed, that $B_{\theta,int}$ has remarkable properties. For example, for any value of θ this component reduces to zero for $R = (5/6)^{½} r_0 = 0.9129 r_0$. As a consequence, $B_{R,int}$ is the only surviving component in this case, so that the direction of $\mathbf{B}_{int}$ is then always perpendicular to the surface of the sphere. In addition, $B_{\theta,int}$ of (4.2) reduces to $+M\sin\theta/r_0^3$ for $R = r_0$ and to $-M\sin\theta/r_0^3$ for $R = (2/3)^{½} r_0 = 0.8165 r_0$.

Combination of (4.1) and (4.2) yields the following general relation for field $\mathbf{B}_{int}$ for the interval $0 \le R \le r_0$

$$\mathbf{B}_{int} = \frac{6\mathbf{M}}{r_0^3}\left(1 - \frac{R^2}{r_0^2}\right) + \left(\frac{3\mathbf{M}\cdot\mathbf{R}}{r_0^5}\mathbf{R} - \frac{\mathbf{M}}{r_0^3}\right). \tag{4.3}$$

Although this general relation follows from the postulated vector potential $\mathbf{A}_{int}$ of (2.1) (see (2.2) for $A_{\varphi,int}$), several limiting cases can rigorously be deduced. For example, the formula for the axial gravitomagnetic field $\mathbf{B}_{int,ax}$ from (3.10b) follows from (4.3). As a consequence, both the expression for the field in the centre of the sphere $\mathbf{B}_c$ and the polar field $\mathbf{B}_p$ in (3.11) follow from (4.3).

Moreover, for the equatorial field $\mathbf{B}_{int,eq}$ follows from (4.3)

$$\mathbf{B}_{int,\,eq} = \frac{5\mathbf{M}}{r_0^3}\left(1 - \frac{6}{5}\frac{R^2}{r_0^2}\right) = \frac{-\beta G^{½} m\boldsymbol{\omega}}{c\,r_0}\left(1 - \frac{6}{5}\frac{R^2}{r_0^2}\right). \tag{4.4}$$

This result can also more directly be calculated from (1.8b) and (2.13). In addition, $\mathbf{B}_{int,eq}$ reduces to the ideal dipole result for $R = r_0$

$$\mathbf{B}_{int,\,eq} = -\frac{\mathbf{M}}{r_0^3} = \frac{\beta G^{½} m\boldsymbol{\omega}}{5c\,r_0}. \tag{4.5}$$

Alternatively, one may start from the truncated series expansion for $A_{\varphi,eq}$ of (2.10). This results applies to the whole interval from $R = 0$ to $R \to \infty$. By applying (1.8b) to (2.10) the corresponding truncated series expansion of the equatorial gravitomagnetic field $\mathbf{B}_{\text{eq}}$ has previously been obtained [15]. In addition, in this work graphical representations of $\mathbf{B}_{\text{eq}}$, corresponding to, e.g., term *T1*, sum *S* for $A_{\varphi,\text{eq}}$ and the present figure 2, have been given. Utilizing (1.8b) a series expansion for $\mathbf{B}_{\text{int,eq}}$, up to terms in $(R/r_0)^6$, can be obtained from (2.12) for the interval $0 \le R \le r_0$

$$\mathbf{B}_{\text{int, eq}} = \frac{5\mathbf{M}}{r_0^3}\left(1-\frac{22}{5}\frac{R^2}{r_0^2}\right) = \frac{-\beta G^{1/2} m\boldsymbol{\omega}}{c r_0}\left(1-\frac{22}{5}\frac{R^2}{r_0^2}\right). \tag{4.6}$$

Note that only terms in $(R/r_0)^0$ and $(R/r_0)^2$ survive. In a series expansion more extended than $A_{\varphi,\text{eq}}$ in (2.12) the value of the coefficient 22/5 in (4.6) will reduce to a lower value, perhaps to the coefficient 6/5 in (4.4). Since the calculation of such an extension is too cumbersome, it has not been carried out. The difference between (4.4) and (4.6) reflects our uncertainty, although the coefficient might even be lower than 6/5.

For the limiting case $R \to \infty$, application of (1.8b) to the truncated series expansion for $A_{\varphi,\text{eq}}$ of (2.10) leads to the following expression for the external, equatorial field $\mathbf{B}_{\text{ext,eq}}$

$$\mathbf{B}_{\text{ext, eq}} = -\frac{\mathbf{M}}{R^3} = \frac{\beta G^{1/2} m\, r_0^{\,2}\boldsymbol{\omega}}{5cR^3}. \tag{4.7}$$

This relation coincides with the required ideal dipole result from (1.11)

The validity of (4.3) can be tested in another way. Utilizing (1.4) and (2.9b), it can be shown, that the components $B_{R,\text{int}}$ of (4.1) and $B_{\theta,\text{int}}$ of (4.2) are solutions of the basic gravitomagnetic equations (1.1). *In this way, the validity of the new formula (4.3) is confirmed!*

5. CALCULATION OF B_θ FOR $R = r_0$, USING STOKES' THEOREM

As an alternative method to calculate the component B_θ of the gravitomagnetic field $\mathbf{B}$ for $R = r_0$, one may use Stokes' theorem. We consider a mass current $\rho\mathbf{v}$ in (1.1a) flowing through a surface bounded by the closed curve *OABCO* denoted in figure 4. Application of Stokes' theorem to (1.1a) to this surface yields

$$\oiint (\nabla\times\mathbf{B})\cdot d\mathbf{S} = \oint \mathbf{B}\cdot d\mathbf{s} = \int_O^A \mathbf{B}\cdot d\mathbf{s} + \int_A^B \mathbf{B}\cdot d\mathbf{s} + \int_B^C \mathbf{B}\cdot d\mathbf{s} + \int_C^O \mathbf{B}\cdot d\mathbf{s} = -\frac{3\beta G^{1/2} m}{c r_0^3}\int \mathbf{v}\cdot d\mathbf{S}, \tag{5.1}$$

where (2.9b) has been used to rewrite the right hand side of (5.1). Note that the directions of the velocity $\mathbf{v}$ and the surface element $d\mathbf{S}$ coincide.

Utilizing the rigorous result for the internal, axial gravitomagnetic field $\mathbf{B}_{\text{int,ax}}$ gravitomagnetic field of (3.10), relation (5.1) can further be evaluated. One obtains

$$\int_A^B \mathbf{B}\cdot d\mathbf{s} + \int_B^C \mathbf{B}\cdot d\mathbf{s} + \frac{8M}{r_0^2} = -\frac{3\beta G^{1/2} m\omega}{c r_0^3}\int_0^\pi \sin\theta d\theta \int_0^{r_0} R^2 dR = -\frac{2\beta G^{1/2} m\omega}{c} = \frac{10M}{r_0^2}. \tag{5.2}$$

Note that the integrations over the intervals *OA* and *CO* are equal. The two integrations left in (5.2) have to be carried out over the semi-circle *ABC* with radius r_0. They can be calculated by introduction of the B_θ component of the gravitomagnetic field $\mathbf{B}$ for $R = r_0$. Equation (5.2) then transforms into

$$\int_0^\pi B_\theta r_0\, d\theta = \frac{2M}{r_0^2}. \tag{5.3}$$

Different expressions for B_θ may be compatible with (5.3). For example, the following one is possible

$$B_\theta = \frac{M \sin\theta}{r_0^3}. \tag{5.4}$$

This relation for B_θ agrees with relation (1.10), representing the field of the ideal gravitomagnetic dipole. It is noticed that a related application of Stokes' theorem has previously been given [15] for a closed surface outside the sphere.

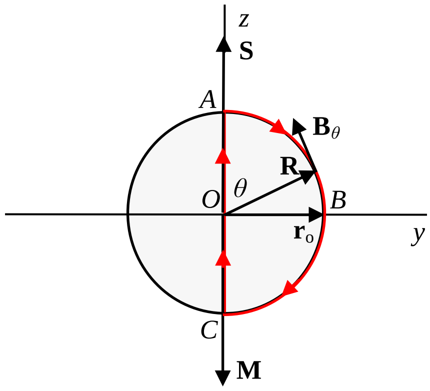

Figure 4. Application of Stokes' theorem to the closed red curve *OABCO* in the *y-z* plane through the centre of the sphere *O*. **S** denotes the angular momentum of the sphere and **M** is its gravitomagnetic moment. The angle between **S** and the position vector **R** is denoted by θ. $\mathbf{B}_\theta$ is the θ-component of the gravitomagnetic field **B** along the semi-circle *ABC* with radius r_0. The red arrows denote the direction of the line elements $d\mathbf{s}$ in which the closed curve is traversed.

It is stressed that alternatives to relation (5.4) are mathematically possible. As an arbitrary example, the following possibility is chosen

$$B_\theta = \left\{1 + a\left(\frac{R}{r_0}\right)^n - \tfrac{3}{2} a \left(\frac{R}{r_0}\right)^n \sin^2\theta\right\} \frac{M \sin\theta}{r_0^3}, \tag{5.5}$$

where a is a dimensionless constant. It has previously been calculated [15] that terms up to $(R/r_0)^6$ cancel, but higher order terms like $(R/r_0)^n$ with $n \geq 7$ might contribute to B_θ. It can easily be shown, that B_θ of (5.5) also satisfies to (5.3). In the limiting case $R = r_0$ and $\theta = 90°$, (5.5) reduces to

$$B_\theta = \left(1 - \tfrac{1}{2} a\right) \frac{M}{r_0^3}. \tag{5.6}$$

For a positive or negative value of a the field B_θ deviates from the ideal dipole result of (5.4). In view of the truncation of the series expansion of (2.10), such a deviation cannot be excluded for the field B_θ calculated in this section.

6. THE ELECTROMAGNETIC VECTOR POTENTIAL A(em) AND THE ELECTROMAGNETIC FIELD B(em)

Analogous to (1.1), the electromagnetic field $\mathbf{B} = \mathbf{B}$(em) in the stationary case can be obtained from the following Maxwell equations (see, e.g., [9, § 26 and § 30])

$$\nabla \times \mathbf{B} = 4\pi c^{-1}\rho_e \mathbf{v} \quad \text{and} \quad \nabla \cdot \mathbf{B} = 0, \tag{6.1}$$

where **v** is velocity and ρ_e is the density of a charge element $dq = \rho_e\, dV$. Comparison of (1.1) and (6.1) shows that the factor $-\beta G^{1/2}\rho$ has been replaced by $+\rho_e$. Note that **B** = **B**(em) has the dimension of a magnetic induction field.

Since $\nabla.\mathbf{B} = 0$, the field **B** can be derived from an electromagnetic vector potential **A** = **A**(em) ($\mathbf{B} = \nabla\times\mathbf{A}$). For a rotating sphere with angular momentum **S** and homogeneous charge density, one finds analogously to (1.2) and (1.5) for $R \geq r_0$ (see, e.g., Landau and Lifshitz [9, § 43 and § 44]))

$$\mathbf{A} = \frac{Q}{2mc}\frac{\mathbf{S}\times\mathbf{R}}{R^3} = \frac{\mathbf{M}\times\mathbf{R}}{R^3}, \tag{6.2}$$

where Q is the total charge and m the total mass of the sphere, respectively. The electromagnetic dipole moment **M** = **M**(em) is given by

$$\mathbf{M} = \tfrac{1}{2}c^{-1}m^{-1}Q\,\mathbf{S}. \tag{6.3}$$

Comparison of the corresponding dipole moments **M**(gm) of (1.4) and **M**(em) of (6.3), respectively, shows that the following transformation has been carried out

$$-\beta G^{1/2} m \rightarrow +Q. \tag{6.4}$$

Utilizing (6.4), the corresponding electromagnetic analogues for A_R, A_θ and A_φ can be found from (1.7). Following the same method, the corresponding values for B_R, B_θ and B_φ can be found from (1.8), (1.9) and (1.10), whereas the formula for **B** of (1.11) remains formally unchanged.

Analogously to (2.1), the internal (i.e., $0 \leq R \leq r_0$) electromagnetic vector potential **A**(em) of the sphere, $\mathbf{A}_{\rm int}$(em), can be found

$$\mathbf{A}_{\rm int}(\text{em}) = \frac{Q}{2mc}\frac{\mathbf{S}\times\mathbf{R}}{R^3}\left(\frac{5}{2} - \frac{3}{2}\frac{R^2}{r_0^2}\right) = \frac{\mathbf{M}\times\mathbf{R}}{r_0^3}\left(\frac{5}{2} - \frac{3}{2}\frac{R^2}{r_0^2}\right). \tag{6.5}$$

Utilizing (6.4), the corresponding electromagnetic analogues for $A_{\varphi,\rm int}$ follows from (2.2) and (2.3).

In order to obtain the truncated series expansion for the electromagnetic component A_φ(em) of the sphere for the whole interval from $R = 0$ to $R \rightarrow \infty$, the methods of sections 2 and 3 can be applied. The equatorial component $A_{\varphi,\rm eq}$(em) can be obtained from the corresponding expression $A_{\varphi,\rm eq}$(gm) of (2.10) by using the transformation of (6.4). The same transformation can be applied to the results in table 1 and the representations in figure 2. Likewise, the results of (3.5), (3.7), (3.9), (3.10) and (3.11) can be transformed by (6.4). Numerical and graphical results for the electromagnetic field **B**(em) can be compared with their gravitomagnetic counterparts given in ref. [15].

Furthermore, the general formula for the internal electromagnetic field of a sphere, denoted by $\mathbf{B}_{\rm int}$(em), formally coincides with its gravitomagnetic counterpart (4.3)

$$\mathbf{B}_{\rm int}(\text{em}) = \frac{6\mathbf{M}}{r_0^3}\left(1 - \frac{R^2}{r_0^2}\right) + \left(\frac{3\mathbf{M}\cdot\mathbf{R}}{r_0^5}\mathbf{R} - \frac{\mathbf{M}}{r_0^3}\right). \tag{6.6}$$

The equatorial fields $\mathbf{B}_{\rm int,eq}$(em) following from (6.6) for different values of R can explicitly be obtained from (4.4) and (4.5), again by using (6.4). Finally, the component

B_θ of the electromagnetic field $\mathbf{B}$(em) for $R = r_0$, may be calculated by application of Stokes' theorem. The result formally coincides with relation (5.4).

7. PROPERTIES OF THE FIELD B AT DIFFERENT VALUES OF *R*

In this section some remarkable properties of the gravitomagnetic (and electromagnetic) field $\mathbf{B}$ are examined. Firstly, the continuity of the external field $\mathbf{B}$ of (1.11) and the internal field $\mathbf{B}_{\text{int}}$ of (4.3) for $R = r_0$ is considered. Comparison of the expressions for the internal field $B_{R,\text{int}}$ from (4.1) and the external field $B_{R,\text{ext}}$ from (1.9) shows that they coincide for $R = r_0$

$$B_{R,\,\text{int}} = \frac{M\cos\theta}{r_0^3}\left(5 - \frac{3R^2}{r_0^2}\right) = \frac{2M\cos\theta}{r_0^3} = B_{R,\,\text{ext}}. \tag{7.1}$$

The relation $B_{R,\text{int}} = B_{R,\text{ext}}$ also follows directly from (1.1b). Application of the integral equivalent of (1.1b) to a pill-box shaped volume whose top and bottom surfaces dS_{ext} and dS_{int} are parallel to the surface of the sphere, leads to

$$\iiint_V (\nabla\cdot\mathbf{B})dV = \oiint \mathbf{B}\cdot d\mathbf{S} = B_{R,\,\text{ext}}dS_{\text{ext}} - B_{R,\,\text{int}}\,dS_{\text{int}} = 0. \tag{7.2}$$

For an infinitesimally small height of the pill-box is $dS_{\text{ext}} = dS_{\text{int}}$. From (7.2) then follows that $B_{R,\text{ext}} = B_{R,\text{int}}$.

Furthermore, the values for the internal field $B_{\theta,\text{int}}$ from (4.2) and the external field $B_{\theta,\text{ext}}$ of (1.10) coincide for $R = r_0$

$$B_{\theta,\,\text{int}} = \frac{M\sin\theta}{r_0^3}\left(-5 + \frac{6R^2}{r_0^2}\right) = \frac{M\sin\theta}{r_0^3} = B_{\theta,\,\text{ext}}. \tag{7.3}$$

In this case the relation $B_{\theta,\text{int}} = B_{\theta,\text{ext}}$ also follows from (1.1a). For a suitable, closed curve *ABCDA* across the boundary of the sphere the quantity $\nabla\times\mathbf{B}$ in (1.1a) approaches to zero value. *A* and *B* are points inside the sphere at distance ds_{int}, whereas *C* and *D* are the corresponding points outside the sphere at distance ds_{ext}. Application of Stokes' theorem to the curve *ABCDA* leads to

$$\oiint (\nabla\times\mathbf{B})\cdot d\mathbf{S} = \oint \mathbf{B}\cdot d\mathbf{s} = B_{\theta,\,\text{int}}ds_{\text{int}} - B_{\theta,\,\text{ext}}ds_{\text{ext}} \to 0. \tag{7.4}$$

For infinitesimally small distances $AB = ds_{\text{int}}$, BC, $CD = ds_{\text{ext}}$ and DA it follows that $BC = DA \to 0$ and $ds_{\text{ext}} \to ds_{\text{int}}$, so that $B_{\theta,\text{int}} \to B_{\theta,\text{ext}}$.

Summing up, the values for the internal field $B_{R,\text{int}}$ from (4.1) and the external field $B_{R,\text{ext}}$ of (1.9) coincide for $R = r_0$. In addition, the values for the internal field $B_{\theta,\text{int}}$ from (4.2) and the external field $B_{\theta,\text{ext}}$ of (1.10) also coincide for $R = r_0$. These results are consistent with the basic relations (1.1b) and (1.1a), respectively.

Secondly, additional remarkable properties of the deduced gravitomagnetic (and electromagnetic) field $\mathbf{B}$ can be illustrated by figure 5. For large values of R the external gravitomagnetic field coincides with the results of the ideal dipole model (see (1.9), (1.10) and (1.11)). Previously, it has been shown [15] that for the polar gravitomagnetic field $B_{\text{p}} = B_R$ of (1.9) ($\theta = 0^\text{o}$) applies from $R = r_0$ to $R \to \infty$. In sections 4 and 5 the deviation of the external gravitomagnetic field $B_{\theta,\text{ext}}$ for $R = r_0$ from the ideal dipole result of (1.10) is checked. Note that within the sphere the field patterns of panels **a** and **b** widely differ, whereas they may coincide for $R \geq r_0$. The corresponding electromagnetic fields $\mathbf{B}$(em) yield analogous field pattern.

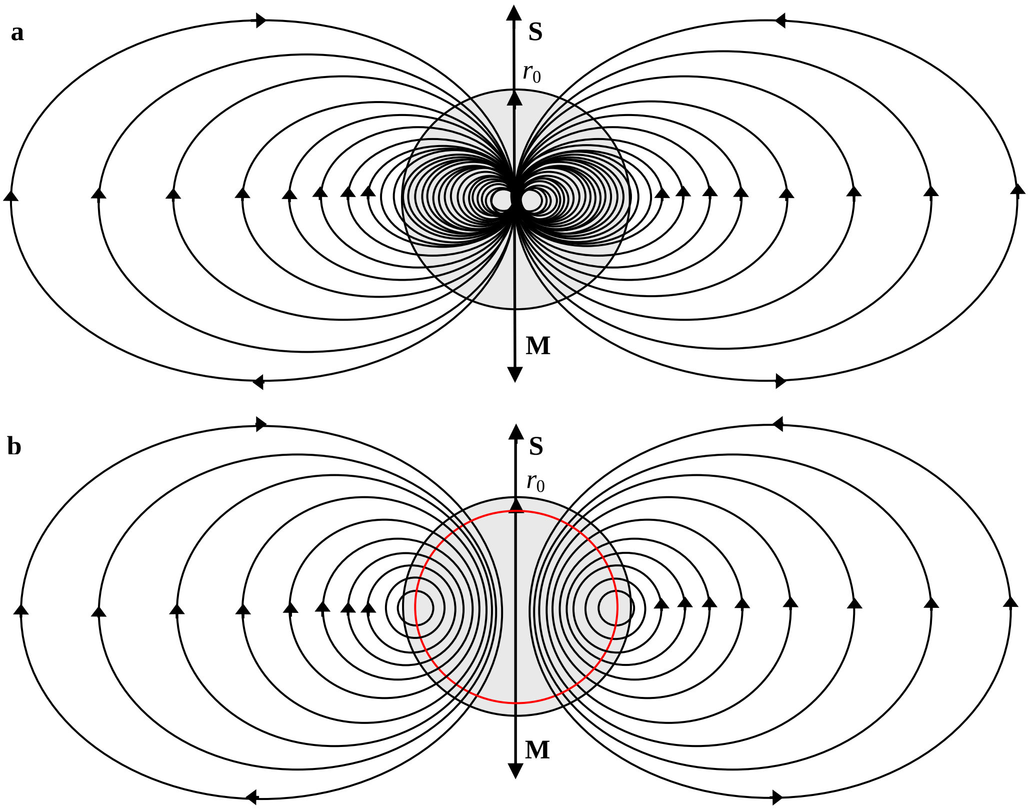

Figure 5. Sketch of the field lines of **B**(gm) from an ideal gravitomagnetic dipole moment **M**, located at the centre of a sphere with radius r_0 (panel **a**). A more accurate picture of the field lines of **B**(gm), inspired by the relations (4.1), (4.2) and (4.3), is given in panel **b**. For the red circle with radius $R = (5/6)^{½} r_0 = 0.9129 r_0$ the component $B_{\theta,\mathrm{int}}$ of (4.2) is zero for any value of θ. Then $B_{R,\mathrm{int}}$ of (4.1) is the only surviving component of $\mathbf{B}_{\mathrm{int}}$. For convenience sake, polar field lines are omitted.

The general internal gravitomagnetic field $\mathbf{B}_{\mathrm{int}}$ is given by (4.3). The component $B_{\theta,\mathrm{int}}$ of (4.2) has remarkable properties. For example, for any value of θ this component reduces to zero for $R = (5/6)^{½} r_0 = 0.9129 r_0$. As a result, in this case $B_{R,\mathrm{int}}$ of (4.1) is the only surviving component. The direction of $\mathbf{B}_{\mathrm{int}}$ is then always perpendicular to the surface of the sphere. Moreover, for values R much smaller than r_0 the ideal dipole model completely fails. In that case, the latter model predicts the wrong sign and magnitude for the field $B_{\theta,\mathrm{int}}$ (compare (1.10) with (4.2)).

8. COMPARISON WITH OBSERVATIONS AND CONCLUSIONS

A comparison between observed and predicted Lense-Thirring precession rates for the LAGEOS/LAGEOS 2 satellites in orbits with $R \approx 1.9 r_0$ around the Earth have been given by Ciufolini *et al.* [10–13]. Likewise, the gravitomagnetic precession rates of four gyroscopes in the Gravity Probe B spacecraft in a polar orbit with $R \approx 1.1 r_0$ around the Earth have reported in 2011 by Everitt *et al.* [14]. All observations are in reasonable agreement with Earth's gravitomagnetic field **B** of (1.11), derived from the ideal dipole model. A discussion of the results of both missions have been given by Biemond [15].

In addition, Bosi *et al.* [16] are preparing an underground ring-laser experiment for the measurement of the local gravitomagnetic field **B**. Using a tri-axial laser detector, they are trying to separate the gravitomagnetic precession rate and geodetic precession rate of the light probe from Earth's rotation rate. It is the aim of their experiment to test the validity of the external field **B** of (1.11), deduced from the ideal dipole model.

It has previously been proposed [5−7, 15, 17−19], that the gravitomagnetic field **B** = **B**(gm), generated by rotating mass and the electromagnetic field **B**(em), due to moving charge may be equivalent. Indications for this equivalence are the approximate validity of the so-called Wilson-Blackett law (for a review, see ref. [5, 6] and references therein; for pulsars, see [17]). In addition, this special interpretation of the gravitomagnetic field results in the deduction of four gravitomagnetic precession frequencies, which have been identified with observed low frequency QPOs for four pulsars and two black holes [18, 19]. Predictions of the proposed model are compatible with observed low frequency QPOs of the pulsars SAX J1808.4−3658, XTE J1807−294, IGR J00291+5934 and SGR 1806−20. For the stellar black hole XTE J1550−564 and the supermassive black hole Sgr A* similar conclusions could be drawn. Although the proposed interpretation is in contradiction with the results reported from Gravity Probe B and LAGEOS satellites, the cited observations also wait for an explanation.

Apart from the equivalence question of the fields **B**(gm) and **B**(em), the deduction of the gravitomagnetic vector potential **A**(gm) and gravitomagnetic field **B**(gm) for a sphere with homogeneous mass density have their own interest. The main results in red of this work are the internal (i.e., $0 \le R \le r_0$), gravitomagnetic vector potential $\mathbf{A}_{\rm int}$ of (2.1) and the corresponding gravitomagnetic field $\mathbf{B}_{\rm int}$ of (4.3). For field points lying on the rotation axis of the sphere a rigorous derivation for the internal axial gravitomagnetic field $\mathbf{B}_{\rm int,\,ax}$ of (3.10) is obtained for the first time. The validity of the general internal field $\mathbf{B}_{\rm int}$ of (4.3) is confirmed at the end of section 4.

It appears that the θ-component of this internal field $\mathbf{B}_{\rm int}$ has remarkable properties. For example, for any value of θ this component $B_{\theta,\,\rm int}$ reduces to zero for $R = (5/6)^{½} r_0 = 0.9129 r_0$. As a consequence, the radial component $B_{R,\,\rm int}$ is the only surviving component in this case. The direction of $\mathbf{B}_{\rm int}$ is then always perpendicular to the surface of the sphere. In addition, $B_{\theta,\,\rm int}$ of (4.2) reduces to $+M\sin\theta/r_0^{\,3}$ for $R = r_0$ and to $-M\sin\theta/r_0^{\,3}$ for $R = (2/3)^{½} r_0 = 0.8165 r_0$.

Starting from a rotating circular torus with homogeneous mass density, truncated series expansions for the vector potential **A**, the component A_φ and the gravitomagnetic field **B** of a rotating sphere have recently been calculated [15] for the whole interval from $R = 0$ to $R \to \infty$. In section 2 the series expansion for the internal equatorial component $A_{\varphi,\,\rm eq}$ has been compared with the corresponding component $A_{\varphi,\,\rm eq}$ of the postulated vector potential $\mathbf{A}_{\rm int}$. Since the series expansion is truncated, only partial agreement is obtained. For the limiting case $R \to \infty$, however, the series expansions for both the external gravitomagnetic vector potential **A** and the external gravitomagnetic field **B** coincide with the ideal dipole results **A** of (1.5) of **B** of (1.11), respectively.

Since observational tests are often carried out near or at the surface of the sphere, special attention is paid to the validity of the ideal dipole model for $R = r_0$. For the polar gravitomagnetic field $\mathbf{B}_{\rm p}$ there is no problem: it is equal to the ideal dipole result of (3.11b). From the general formula (4.3) for the internal gravitomagnetic field $\mathbf{B}_{\rm int}$, confirmed at the end of section 4, it also follows that the field $\mathbf{B}_{\rm int}$ always coincides with the ideal dipole field for $R = r_0$. Using Stokes' theorem, it is shown in section 5 that the θ-component $B_{\theta,\,\rm int}$ of the internal field $\mathbf{B}_{\rm int}$ is compatible with the ideal dipole result (5.4). It is demonstrated, however, that a deviation from the latter result cannot be excluded in that approach.

In addition, for a rotating sphere with homogeneous charge density the electromagnetic vector potential **A**(em) and the electromagnetic field **B**(em) follow from the Maxwell equations. Expressions for the internal fields $\mathbf{A}_{\rm int}$(em) and $\mathbf{B}_{\rm int}$(em), analogous to the gravitomagnetic case, are given and discussed in section 6.

In conclusion, the more detailed deduction of the gravitomagnetic (and electromagnetic) vector potential **A** and the gravitomagnetic field **B** of a rotating sphere with homogeneous mass density may be helpful in many future applications.

REFERENCES

[1] Heaviside, O., "A gravitational and electromagnetic analogy." In: *Electromagnetic Theory*, 3rd ed., Chelsea Publishing Company, New York, vol. I, app B, pp. 455-466 (1971) (1st ed. at London in 1922).

[2] Singh, A., "Quaternionic form of linear equations for the gravitational field with Heavisidian monopoles." *Lett. Nuovo Cim.* **32**, 5-8 (1981) and ref. [5] therein.

[3] Cattani, D. D., "Linear equations for the gravitational field." *Nuovo Cim.B.* **60**, 67-80 (1980).

[4] Peng, H., "On calculation of magnetic-type gravitation and experiments." *Gen. Rel. Grav.* **15**, 725-735 (1983).

[5] Biemond, J., *Gravito-magnetism*, 2nd ed. (1999). Postal address: Sansovinostraat 28, 5624 JX Eindhoven, The Netherlands. E-mail: j.biemond@gravito.nl Websites: http://www.gravito.nl and http://www.gewis.nl/~pieterb/gravi/

[6] Biemond, J., *Gravi-magnetism*, 1st ed. (1984). See also Ref. [5].

[7] Biemond, J., "Which gravitomagnetic precession rate will be measured by Gravity Probe B?" arXiv:physics/0411129v1 [physics.gen-ph], 13 Nov 2004.

[8] Ruggiero, M. L. and Tartaglia, A., "Gravitomagnetic effects." *Nuovo Cim. B* **117**, 743-767 (2002).

[9] Landau, L. D. and Lifshitz, E. M., *The classical theory of fields*, 4th rev. ed., Pergamon Press, Oxford (1975).

[10] Ciufolini, I., Lucchesi, D., Vespe, F. and Mandiello, A., "Measurement of dragging of inertial frames and gravitomagnetic field using laser-ranged satellites." *Nuovo Cim. A* **109**, 575-590 (1996).

[11] Ciufolini, I., "On a new method to measure the gravitomagnetic field using two orbiting satellites." *Nuovo Cim. A* **109**, 1709-1720 (1996).

[12] Ciufolini, I. and Pavlis, E. C., "A conformation of the general relativistic prediction of the Lense-Thirring effect." *Nature* **431**, 958-960 (2004).

[13] Ciufolini, I., "Dragging of inertial frames." *Nature* **449**, 41-47 (2007).

[14] Everitt, C. W. F., DeBra, D. B., Parkinson, B. W., *et al.* "Gravity Probe B: Final results of a space experiment to test general relativity." *Phys. Rev. Lett.* **106**, 221101-1-5 (2011).

[15] Biemond, J., "The gravitomagnetic field of a sphere, Gravity Probe B and the LAGEOS satellites." arXiv:physics/0802.3346v2 [physics.gen-ph], 14 Jan 2012.

[16] Bosi, F., Cella, G., Di Virgilio, A. Ortolan, A., Porzio, A., Solimeno, S., Cerdonio, M., Zendri, J. P., Allegrini, M., Belfi, J., Beverini, N., Bouhadef, B., Carelli, G., Ruggiero, M. L., Tartaglia, A., Schreiber, K. U., Gebauer, A. and Wells, J-P. R. "Measuring gravito-magnetic effects by multi ring-laser gyroscope." *Phys. Rev D* **84**, 122002 (2012).

[17] Biemond, J., "The origin of the magnetic field of pulsars and the gravitomagnetic theory." In: *Trends in pulsar research* (Ed. Lowry, J. A.), Nova Science Publishers, New York, ch. 2 (2007) (updated and revised version of arXiv:astro-ph/0401468v1, 22 Jan 2004).

[18] Biemond, J., "Quasi-periodic oscillations, charge and the gravitomagnetic theory." arXiv:0706.0313v2 [physics.gen-ph], 20 Mar 2009.

[19] Biemond, J., "Quasi-periodic oscillations, mass and jets of black holes: XTE J1550−564 and Sgr A*." viXra: astrophysics/1001.0021v1, 18 Jan 2010.

[20] Jackson, J. D., *Classical electrodynamics*, 2nd ed., John Wiley & Sons, New York, ch. 5 (1975).

[21] Gradshteyn, I. S. and Ryzhik, I. M., *Tables of integrals, series, and products*, 5th ed., (Ed. Jeffrey, A.), Academic Press, Boston (1994).